

# A Detrimental Reaction at the Molybdenum Back Contact in $\text{Cu}_2\text{ZnSn}(\text{S},\text{Se})_4$ Thin-Film Solar Cells

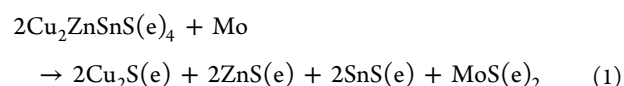
Jonathan J. Scragg,\* J. Timo Wätjen, Marika Edoff, Tove Ericson, Tomas Kubart, and Charlotte Platzer-Björkman

Ångström Solar Center, Solid State Electronics, Uppsala University, 751 21 Uppsala, Sweden

**S** Supporting Information

**ABSTRACT:** Experimental proof is presented for a hitherto undetected solid-state reaction between the solar cell material  $\text{Cu}_2\text{ZnSn}(\text{S},\text{Se})_4$  (CZTS(e)) and the standard metallic back contact, molybdenum. Annealing experiments combined with Raman and transmission electron microscopy studies show that this aggressive reaction causes formation of  $\text{MoS}_2$  and secondary phases at the CZTS|Mo interface during thermal processing. A reaction scheme is presented and discussed in the context of current state-of-the-art synthesis methods for CZTS(e). It is concluded that alternative back contacts will be important for future improvements in CZTS(e) quality.

The kesterite materials  $\text{Cu}_2\text{ZnSn}(\text{S},\text{Se})_4$  (abbreviated to CZTS(e)) promise a new generation of thin-film solar cells based on earth-abundant, low-toxicity elements. To date, the record CZTS(e) solar cell efficiency stands at 11.1%.<sup>1</sup> However, for kesterite-based solar cells to contend with their indium-containing predecessor,  $\text{Cu}(\text{In},\text{Ga})\text{Se}_2$  (CIGS), this value must be roughly doubled.<sup>2</sup> Key to achieving this goal is a detailed understanding of the chemical processes occurring during synthesis of CZTS(e). It is already known that surface decomposition of CZTS(e) can occur during thermal processing—especially when low pressures are used—resulting in loss of S(e) and SnS(e). This surface decomposition is enabled by the relatively facile reduction of Sn(IV) to Sn(II) in a chalcogen environment, which is an inherent characteristic of Sn chemistry.<sup>3</sup> In the present Communication, we point out a further consequence of this instability, which causes us to doubt the suitability of molybdenum (Mo) as a standard “back contact” layer for CZTS(e). The back contact is a conductive layer used to make electrical contact to the underside of the solar cell. For CIGS, Mo is chosen because it is relatively inert and has suitable electronic properties. The CIGS layer is normally deposited directly onto a Mo-coated substrate, and the same approach has been widely adopted for CZTS(e). However, a thermodynamic analysis suggests that the CZTS(e)|Mo interface may not be as chemically stable as the CIGS|Mo interface. During thermal processing, which is a necessary step in fabrication of high-efficiency devices, the favorability of  $\text{MoS}(\text{e})_2$  formation combined with the aforementioned ease of reduction of Sn(IV) could lead to removal of S(e) from CZTS(e) at the back contact, inducing phase segregation:



Using a method highlighted recently,<sup>4</sup> we calculate the free energy change of reaction 1 to be around  $-100$  kJ for CZTSe and  $-150$  kJ for CZTS at  $550$  °C, a typical anneal temperature. The full calculations are given in Appendix 1 in the Supporting Information. Such negative free energy changes are a strong driving force for reaction 1, implying that the CZTS(e)|Mo interface is unstable. In contrast, the equivalent reaction for CIGS has a positive free energy change: CIGS is by nature stable on a Mo substrate.<sup>4</sup>

Thermodynamic calculations alone cannot prove that reaction 1 really occurs, because there is an activation barrier of unknown magnitude; experimental input is thus required. The current literature shows that rather thick  $\text{MoS}(\text{e})_2$  layers are common after annealing. However, since CZTS(e) is in most cases annealed in a S(e) ambient, the contribution of reaction 1, if any, to  $\text{MoS}(\text{e})_2$  formation is impossible to distinguish. At the same time, a variety of secondary phases have been reported at the back contact, including  $\text{ZnS}$ ,<sup>5,6</sup>  $\text{Sn}_x\text{S}_y$ ,<sup>7</sup> and  $\text{Cu}_x\text{SnS}_y$ .<sup>6</sup> Although the location of these phases suggests a back contact process, the actual phases observed are often different from those predicted by reaction 1.

In this Communication, we provide proof that reaction 1 does indeed occur, leading us to conclude that the CZTS(e)|Mo interface is unstable during annealing. We present a reaction scheme that can naturally explain the literature observations of different secondary phases at the back contact, and we discuss some of the implications of reaction 1 for developing better synthesis processes and, ultimately, more efficient CZTS(e) solar cells.

Here we report annealing studies designed to test the existence of reaction 1 in the CZTS (sulfide) case. The precursors used for annealing experiments were reactively sputtered CZTS films, deposited on Mo-coated soda lime glass substrates at around  $180$  °C. The rapid re-crystallization of these precursors upon annealing is discussed elsewhere.<sup>8</sup> Full details of all preparation and characterization procedures are included in the Supporting Information.

We highlight the two key predictions of reaction 1, which should both be seen when annealing the CZTS|Mo samples:

- (i)  $\text{MoS}_2$  should grow at the CZTS|Mo interface.

Received: September 6, 2012

Published: November 12, 2012

(ii) Phase separation into  $\text{Cu}_2\text{S}$ ,  $\text{ZnS}$ , and  $\text{SnS}$  should occur at the back contact.

To confidently attribute the above observations to reaction 1, we must carefully eliminate all other processes that could lead to the same phenomena. To begin with, point (i) requires that we eliminate all other S sources that could cause growth of  $\text{MoS}_2$ , otherwise the origin of the  $\text{MoS}_2$  would be unclear. As we have previously described, the as-sputtered precursors have stoichiometric S content and do not contain a measurable excess of S.<sup>9</sup> We checked also that  $\text{MoS}_2$  was not generated during the reactive sputtering: Raman spectra recorded on the back contact after removal of the CZTS precursor layer are identical to spectra from fresh Mo substrates. Residual S vapor in the anneal system could also cause  $\text{MoS}_2$  growth. To minimize the S background in the annealing system, it was heated to 600 °C under vacuum for 12 h. A bare Mo sample was then annealed for 60 min. Raman spectroscopy revealed extremely weak bands matching  $\text{MoS}_2$ ,<sup>10</sup> but no layer could be resolved by scanning electron microscopy (SEM). From this we estimate that the  $\text{MoS}_2$  layer was less than 5 nm thick. As we will shortly see, this is a negligible contribution for the present study. The Raman spectra mentioned above are included as Supporting Information.

Point (ii) concerns the formation of secondary phases. The simultaneous occurrence at the back contact of the secondary phases predicted by reaction 1 would be difficult to explain by another process, but we can nonetheless remove possible ambiguity by limiting all other processes that could lead to secondary phases. This requires that the CZTS layer should be homogeneous and as close to stoichiometry as possible in metallic content, to avoid the spontaneous phase segregation expected for non-stoichiometric material.<sup>11</sup> Another potential source of secondary phases is the surface decomposition reaction, which generates  $\text{Cu}_2\text{S}$  and  $\text{ZnS}$  (while  $\text{SnS}$  and S are lost to the vapor phase).<sup>12</sup> Surface stability can be achieved by supplying S and  $\text{SnS}$  vapor;<sup>3</sup> however, doing this would contradict the requirements of point (i). To stabilize the surface as much as possible without adding an external S source, we annealed samples with a glass cover in direct contact with the film, and supplied a static annealing atmosphere of 300 mbar argon. We have determined that a slight Sn excess in the precursor is enough to create a pseudo-equilibrium in the small volume above the CZTS surface. Accordingly, we prepared the precursors with composition  $\text{Cu}/\text{Sn} = 1.77$  and  $\text{Zn}/\text{Sn} = 0.97$ . Upon annealing, evaporation of the excess  $\text{SnS}$  and S into the small volume above the samples keeps the CZTS phase stable. The composition after annealing for 10 min at 560 °C is near-stoichiometric, with  $\text{Cu}/\text{Sn} = 1.92$  and  $\text{Zn}/\text{Sn} = 1.05$ . This places the annealed sample in the single-phase region of the  $\text{Cu}_2\text{S}$ – $\text{ZnS}$ – $\text{SnS}_2$  phase diagram,<sup>11</sup> meaning that no secondary phases should form spontaneously.

SEM cross sections of the 10 min annealed sample (Figure 1) revealed large grains in the bulk phase, and smaller particles at the back contact. The upper 50–60 nm of the Mo layer had a different morphology, the first indication that  $\text{MoS}_2$  had formed. To identify the phases present at different locations in the layer, Raman spectra with a 514 nm excitation wavelength were recorded (a) on the top surface of the CZTS film, (b) on the back surface of the CZTS film—by applying an adhesive tape to the film and separating it from the substrate using a razor blade—and (c) on the thus-exposed Mo substrate. These measurements are shown in Figure 1. The top surface

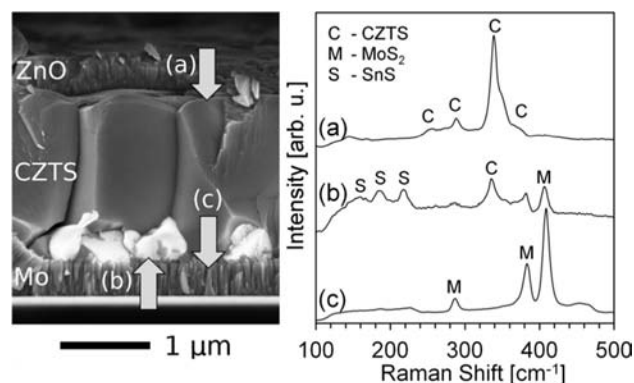


**Figure 1.** Left: SEM image of the 10-min annealed CZTS film (after addition of top layers for solar cell fabrication). Arrows schematically illustrate the locations where Raman spectra, right, were measured: (a) at the surface of the as-annealed CZTS film, (b) at the back surface of the same film, and (c) on the substrate after film removal.

measurements confirm that the bulk material is CZTS—all the expected modes are clearly seen.<sup>5</sup> No secondary phases can be seen within the information depth of the measurement, which is around 150 nm.

Under the optical microscope of the Raman system, the back surface of the CZTS film showed clusters of contrasting material covering an estimated 20% of the sample area (see Supporting Information). When focusing the laser on the clusters, three new bands appeared at 160, 185, and 220  $\text{cm}^{-1}$ , alongside a weaker CZTS response. The new bands are an excellent match to tin monosulfide,  $\text{SnS}$ .<sup>13</sup> Spectra measured on the exposed substrate showed bands corresponding to  $\text{MoS}_2$ ,<sup>10</sup> as anticipated from the SEM image. The most intense  $\text{MoS}_2$  bands are also seen in spectrum (b), showing that a part of the  $\text{MoS}_2$  layer adheres to the CZTS film when it is removed from the substrate. The other products of reaction 1— $\text{Cu}_2\text{S}$  and  $\text{ZnS}$ —are unlikely to be detected with our Raman system,  $\text{Cu}_2\text{S}$  because of its metallic character and  $\text{ZnS}$  because its adsorption is very weak at the excitation wavelength used. Therefore we also employed scanning transmission electron microscopy (STEM) with energy dispersive X-ray spectroscopy (EDS) on cross sections prepared by focussed ion beam milling to help identify the phases at the back contact. In prior work, we have used this technique to show that  $\text{Cu}$ – $\text{S}$ ,  $\text{Zn}$ – $\text{S}$  and  $\text{Sn}$ – $\text{S}$  regions were present at the back contact, although at that time the exact phases were not identified. It was also shown that the coverage of the interface by these phases increased with anneal time.<sup>14</sup> Figure 2 shows a typical cluster of secondary phases and the corresponding elemental maps for the 10 min annealed sample. In this example, regions of  $\text{Sn}$ – $\text{S}$  and  $\text{Zn}$ – $\text{S}$  are shown. The  $\text{Sn}$ – $\text{S}$  regions shown in Figure 2 correspond to the tin monosulfide observed by Raman spectroscopy. The  $\text{Zn}$ – $\text{S}$  and  $\text{Cu}$ – $\text{S}$  regions were confirmed by electron diffraction to be cubic  $\text{ZnS}$  and a  $\text{Cu}_{2-x}\text{S}$  phase (see right side of Figure 2).  $\text{Cu}_{2-x}\text{S}$  particles occurred less frequently than  $\text{ZnS}$  and  $\text{SnS}$ . This could be explained by the well-known mobility of Cu atoms in chalcogenide materials: it is possible that some of the Cu was re-absorbed into the slightly Cu-poor bulk further from the back contact (where  $\text{Cu}/\text{Sn} = 1.92$ ), diminishing the fraction of segregated  $\text{Cu}_{2-x}\text{S}$  phases.

We investigated the rate of  $\text{MoS}_2$  growth by annealing a series of samples for different time periods and measuring the thickness of the  $\text{MoS}_2$  layer. Standard kinetic models for the formation of oxide layers predict a  $t^{1/2}$  dependence of layer

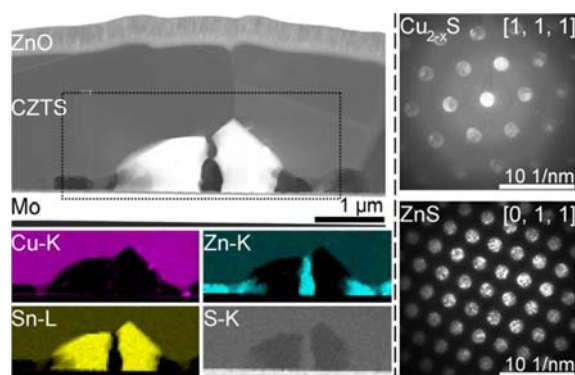


**Figure 2.** Main image: STEM image of the 10-min annealed CZTS film, indicating the area mapped by EDS. Below: EDS maps showing Sn–S and Zn–S grains at the back contact. Right: representative electron diffraction patterns recorded on Cu–S and Zn–S regions, which were thereby identified to be  $\text{Cu}_{2-x}\text{S}$  and cubic ZnS.

thickness, with the reaction slowing as the layer gets thicker because atoms need to diffuse further to reach unreacted material.<sup>15</sup> Our results, as estimated from SEM cross sections, match well to this prediction (see Figure 3). As mentioned, coverage of the back contact by secondary phases also increased with anneal time.<sup>14</sup>

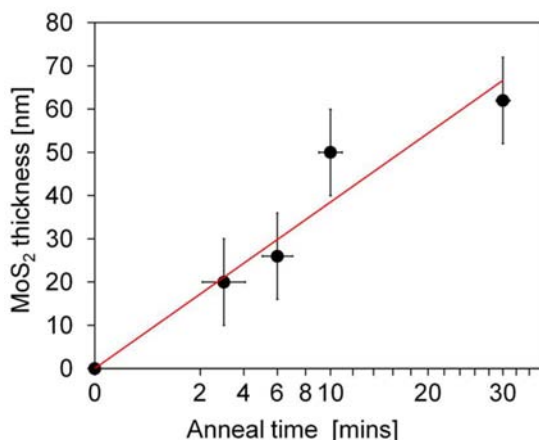


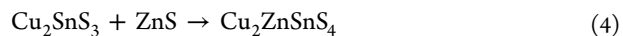
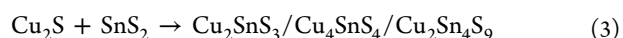
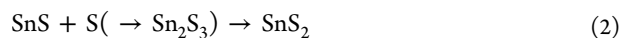
**Figure 3.** Growth of  $\text{MoS}_2$  under CZTS films during annealing without added sulfur, estimated from SEM cross sections. A square-root scale is used to show agreement with theory.

Observation of  $\text{MoS}_2$ ,  $\text{Cu}_{2-x}\text{S}$ , ZnS, and SnS at the back contact is exactly in line with the predictions of reaction 1. However, before reaching any conclusions, we consider some alternative explanations as follows: (A) To begin, it is clear that the 50–60 nm  $\text{MoS}_2$  layer that formed during 10 min of annealing the CZTS film could not have arisen from the residual sulfur vapor in the anneal system (which generated at most 5 nm of  $\text{MoS}_2$  after 60 min of annealing a bare Mo sample). (B) Another S source could be the surface decomposition reaction—responsible for the Sn losses during annealing—which is accompanied by loss of S vapor.<sup>3</sup> This vapor could in principle diffuse to the back contact and cause  $\text{MoS}_2$  growth. However, this could not explain the observed formation of  $\text{Cu}_{2-x}\text{S}$ , ZnS and SnS at the back contact. (C) While the precursors were stoichiometric in S content within the error of the EDS measurement, a few atomic percent sulfur excess could in principle be present.<sup>9</sup> This could explain a part

of the  $\text{MoS}_2$  layer, but is inconsistent with the presence of the S-poor phase SnS (which indicates that the CZTS layer is S-poor, not S-rich), and does not account for the  $\text{Cu}_{2-x}\text{S}$  and ZnS phases. (D) The presence at the back contact of both the reduced and oxidized compounds in reaction 1, namely SnS and  $\text{MoS}_2$ , is a clear sign of S transfer across the CZTS/Mo interface. Another hypothesis consistent with that process is as follows: since the precursor was Sn-rich,  $\text{SnS}_2$  particles could reasonably be expected to segregate.<sup>11</sup> The reaction of  $\text{SnS}_2$  with Mo is also thermodynamically favorable, and would yield SnS and  $\text{MoS}_2$ .<sup>4</sup> However, while this process may occur to some extent, it cannot be the dominant reaction because it is inconsistent with (i) the observation of  $\text{Cu}_{2-x}\text{S}$  and ZnS, and (ii) the fact that the Sn excess was lost from the film during annealing, and therefore cannot be the main source of the SnS particles observed here.

After considering these possibilities, we find that only reaction 1 can completely and without contradiction explain both the growth of the  $\text{MoS}_2$  layer and the occurrence of the observed secondary phases at the back contact. We are therefore able to conclude with confidence that the thermodynamic prediction is accurate: CZTS is not stable when in contact with Mo during thermal processing. We point out that, given the similarity between the sulfide and selenide systems, we have strong grounds to assume that reaction 1 also occurs in the selenide compound CZTSe, and we expect future experiments to confirm this assumption.

We now explore how the situation at the back contact is changed under more typical annealing conditions, i.e., when S (or  $\text{H}_2\text{S}$ ) is supplied. A high partial pressure of S will cause diffusion of S atoms through the CZTS layer, which will have two results: First, it creates an additional mechanism for  $\text{MoS}_2$  growth, causing the rate of reaction 1 to decrease (see explanation of Figure 3). Second, in the presence of excess S, the SnS phase formed by reaction 1 will be re-oxidized, returning to  $\text{SnS}_2$  and allowing regeneration of ternary and quaternary phases as follows:<sup>11,16</sup>



At first sight, therefore, although it will certainly increase the formation rate of  $\text{MoS}_2$ , S annealing appears to completely reverse the phase separation of reaction 1. However, the frequent literature reports of secondary phases at the back contact even after S annealing suggest otherwise. In an important example, ZnS and a Cu–Sn–S phase were seen at the back contact in CZTS layers after sulfur-annealing of co-evaporated precursors—the process used to make the current record pure sulfide CZTS device.<sup>6</sup> We can understand this as follows: in the first stages of annealing, reaction 1 caused phase separation into  $\text{Cu}_2\text{S}$ , ZnS and SnS, and initiated the formation of  $\text{MoS}_2$ . When the supplied sulfur vapor diffused through the CZTS layer to the back contact, reaction 2 occurred. The separated phases were then able to recombine, reactions 3 and 4, but this process did not go to completion within the allowed annealing time. Reasons for the slow rate of reactions 3 and 4 could include a low driving force or spatial separation of the products of reaction 1.

In addition, there is a fundamental limit on the ability of S(e) annealing to combat the back contact reaction. Since diffusion

of S(e) to the back contact must take a finite time, there is always a “window of opportunity”,  $\Delta t$ , at the start of the anneal in which reaction 1 can occur uninhibited. Even a saturation pressure of S(e) could never reduce  $\Delta t$  to zero. The conclusion is that S(e) annealing can reduce the phase separation caused by reaction 1, but cannot stop it from happening in the first place. The greatest effect will be seen at high S(e) pressures, when the rate of S(e) transport to the back contact is maximized. Of course, a side effect of this is that the MoS(e)<sub>2</sub> thickness will be increased. Some of the best-performing CZTS(e) devices have MoS(e)<sub>2</sub> layers of as much as 100–200 nm,<sup>1,6</sup> which shows that rather high S(e) pressures were used during annealing. These thick MoS(e)<sub>2</sub> layers have been implicated in poor adhesion and high series resistance in the solar cell,<sup>17</sup> but this may still be preferable to a situation where phase segregation at the back contact occurs completely unchecked.

It is interesting to consider how the back contact reaction could influence solar cell properties. One adverse effect is that the lower band gap phases generated (SnS(e), Cu<sub>2-x</sub>S(e), and Cu<sub>2</sub>SnS(e)<sub>3</sub>) could enhance recombination of charge carriers near the back contact. However, a potentially more serious consequence arises from the fact that reaction 1 is a phase segregation, where a single phase breaks down into several new phases. Generally speaking, phase segregation occurs because the concentration of a particular crystal defect has exceeded its solubility limit in the single phase. Thus, even before the phase segregation expressed in reaction 1 is observed, the reaction with Mo is presumed to generate defects, likely Sn(II) and S(e) vacancies, within the CZTS(e) single phase. Defects generated at the back contact have the potential to affect the entire CZTS(e) layer by diffusing away from their origin and into the bulk. At present this is a hypothesis: the effect of the back contact reaction on solar cells must be investigated experimentally. Nevertheless, it is undeniably important to eliminate all processes that reduce the quality and uniformity of the CZTS(e) layer if the goal of high efficiency (>15%) solar cells is to be achieved.

Ultimately, because reaction 1 is caused by a chemical incompatibility of CZTS(e) and Mo, eliminating it completely requires either replacement of Mo with a more inert material, or the use of a barrier layer to passivate the interface. We note that there is already some evidence that the latter approach is effective.<sup>17</sup> If an inert back contact can be achieved, then we expect that the formation of secondary phases at the CZTS(e) back contact will be eliminated, and a potential source of defects will be removed. Currently, an inert back contact is a feature of CIGS solar cells that is not shared by CZTS(e). This may be one of the reasons for the lower performance of the latter.

In summary, a reaction has been shown to occur between the solar cell material CZTS and the standard Mo back contact layer. The reaction occurs during thermal processing, resulting in decomposition of the CZTS layer into Cu<sub>2</sub>S, ZnS and SnS, and growth of MoS<sub>2</sub>. The same reaction is expected for the selenide variant, and can explain the variety of secondary phases reported at the back contact. Current synthesis methods appear unable to fully prevent the back contact reaction. On the basis of this, we recommend that the choice of Mo as a standard back contact material in CZTS(e) devices should be urgently re-examined.

## ■ ASSOCIATED CONTENT

### 📄 Supporting Information

Full experimental procedures. This material is available free of charge via the Internet at <http://pubs.acs.org>.

## ■ AUTHOR INFORMATION

### Corresponding Author

[jonathan.scragg@angstrom.uu.se](mailto:jonathan.scragg@angstrom.uu.se)

### Notes

The authors declare no competing financial interest.

## ■ ACKNOWLEDGMENTS

The authors acknowledge support from the Swedish Energy Agency and Carl Trygger Foundation in funding this work.

## ■ REFERENCES

- (1) Todorov, T. K.; Tang, J.; Bag, S.; Gunawan, O.; Gokmen, T.; Zhu, Y.; Mitzi, D. B. *Adv. Energy Mater.* **2012**, DOI: 10.1002/aenm.201200348.
- (2) Jackson, P.; Hariskos, D.; Lotter, E.; Paetel, S.; Wuerz, R.; Menner, R.; Wischmann, W.; Powalla, M. *Prog. Photovolt.: Res. Appl.* **2011**, *19*, 894.
- (3) Scragg, J. J.; Ericson, T.; Kubart, T.; Edoff, M.; Platzer-Bjorkman, C. *Chem. Mater.* **2011**, *23*, 4625.
- (4) Scragg, J. J.; Dale, P. J.; Colombara, D.; Peter, L. M. *ChemPhysChem* **2012**, *13*, 3035.
- (5) Fontane, X.; Calvo-Barrío, L.; Izquierdo-Roca, V.; Saucedo, E.; Perez-Rodriguez, A.; Morante, J. R.; Berg, D. M.; Dale, P. J.; Siebentritt, S. *Appl. Phys. Lett.* **2011**, *98*, 181905.
- (6) Wang, K.; Shin, B.; Reuter, K. B.; Todorov, T.; Mitzi, D. B.; Guha, S. *Appl. Phys. Lett.* **2011**, *98*, 051912.
- (7) Fernandes, P. A.; Salomé, P. M. P.; da Cunha, A. F. J. *Alloys Compd.* **2011**, *509*, 7600.
- (8) Scragg, J. J.; Ericson, T.; Fontané, X.; Izquierdo-Roca, V.; Pérez-Rodríguez, A.; Kubart, T.; Edoff, M.; Platzer-Björkman, C. *Prog. Photovolt.: Res. Appl.* **2012**, DOI: 10.1002/pip.2265.
- (9) Ericson, T.; Kubart, T.; Scragg, J. J.; Platzer-Björkman, C. *Thin Solid Films* **2012**, *520*, 7093.
- (10) Sandoval, S. J.; Yang, D.; Frindt, R. F.; Irwin, J. C. *Phys. Rev. B* **1991**, *44*, 3955.
- (11) Olekseyuk, I. D.; Dudchak, I. V.; Piskach, L. V. *J. Alloys Compd.* **2004**, *368*, 135.
- (12) Redinger, A.; Berg, D. M.; Dale, P. J.; Siebentritt, S. *J. Am. Chem. Soc.* **2011**, *133*, 3320.
- (13) Parkin, I. P.; Price, L. S.; Hibbert, T. G.; Molloy, K. C. *J. Mater. Chem.* **2001**, *11*, 1486.
- (14) Wätjen, J. T.; Scragg, J. J.; Ericson, T.; Edoff, M.; Platzer-Björkman, C. *Thin Solid Films* **2012**, in press.
- (15) Deal, B. E.; Grove, A. S. *J. Appl. Phys.* **1965**, *36*, 3770.
- (16) Hergert, F.; Hock, R. *Thin Solid Films* **2007**, *515*, 5953.
- (17) Shin, B.; Zhu, Y.; Bojarczuk, N. A.; Chey, S. J.; Guha, S. *Appl. Phys. Lett.* **2012**, *101*, 053903.